MADRID
inter.noise 2019
June 16 - 19
NOISE CONTROL FOR A BETTER ENVIRONMENT

Aerodynamic and acoustic optimization of a multi-blade centrifugal fan

Wang, Chen[1]
Northwestern Polytechnical University
127 West Youyi Road, Beilin District, Xi'an, Shaanxi Province, P.R.China

Mai, Kai[2]
Northwestern Polytechnical University
127 West Youyi Road, Beilin District, Xi'an, Shaanxi Province, P.R.China

ABSTRACT

An existing multi-blade centrifugal fan is optimized both aerodynamically and acoustically with numerical methods. The influence of several significant structure parameters on the flow field performance is systematically explored first with ANSYS CFX software, including the number of blades, the inlet and outlet angles of blades, and the gap between the volute and the blade trailing edge near the volute tongue. Noise reduction by improving the flow field performance is expected and this hypothesis is verified through acoustic numerical calculation with the combination of LMS Virtual.Lab Finite Element and Boundary Element Acoustics. In addition, a wideband sound-absorbing volute structure is designed and optimized based on the acoustic simulation result of the previous aerodynamically optimized centrifugal fan. The results suggest that noise can be reduced simply from the perspective of flow field optimization, through the adjustment of key structure parameters. The sound-absorbing structure in volute is effective in centrifugal fan noise control, and the benefit is further improved if the position of this structure is optimized based on the radiation characteristics of the blade rotating noise source and the parameters of this structure is optimized based on the spectral characteristics of the radiated noise.

Keywords: Multi-blade centrifugal fan, Noise control, Sound-absorbing volute
I-INCE Classification of Subject Number: 14

1. INTRODUCTION

As a fluid mechanical structure that converts mechanical energy into wind energy, the multi-blade centrifugal fan is widely used in range hoods, air conditioners, and industrial ventilation equipment. However, the large flow rate and high pressure characteristics of the multi-blade centrifugal fan cause the internal fluid flow to generate relatively considerable fluctuating pressure, and thus obvious noise. The presence of

[1]cwang@nwpu.edu.cn
[2]593304757@qq.com

noise not only causes significant noise pollution to people's living environment, but also has a rather negative impact on the operational performance of the equipment. With the increasing attention to environmental noise problems, requirements for the acoustic performance of centrifugal fans are becoming more and more demanding. Under this background, the aerodynamic noise control of multi-blade centrifugal fans is very meaningful.

The typical design parameters of multi-blade centrifugal fans, including radius of volute tongue, number of impeller blades, blade incidence angle, etc., not only have a significant effect on the internal flow field, but also are closely related to its aerodynamic characteristics and noise levels. Therefore, lots of studies focus on the optimization of these key design parameters to improve the aerodynamic and acoustic performances of multi-blade centrifugal fans[1]. Detailed analysis of the unsteady and three-dimensional flow pattern between the fan blades is made, and the relation between the pressure fluctuation on the blade surfaces and the flow pattern are explored[2-5]. Due to the strong unsteady interaction of the inhomogeneous flow at the exit of rotating impeller blades with the volute, the surface of volute, especially the tongue region, becomes the major noise source area[6]. The induced unsteady force is the main cause of tonal noise component. A vast majority of studies on noise reduction of centrifugal fans concentrate upon the adjustment of volute tongue such as changing the angle of inclination, increasing the impeller blade-tongue clearance[7-10]. These methods can achieve favourable noise reduction effect, though at the cost of impairing the original aerodynamic performance. Thus, the development of measures which can suppress the aerodynamic noise and simultaneously keep (even improve) its original aerodynamic performance becomes one of the targets with regards to the research of fan noise reduction.

This paper is organized as follows. The influences of several key structural parameters of the studied multi-blade centrifugal fan on flow field, aerodynamic performance and radiated noise are analyzed firstly, including blade installation angle, number of impeller blades and volute tongue clearance. Secondly, a novel composite sound absorption structure is designed and optimized, and its sound absorption coefficient is numerically predicted. The influence of the installation position of the designed composite sound absorption structure on noise reduction is analyzed, followed by an acoustic experimental test of the multi-blade centrifugal fan after aerodynamic and acoustic improvement.

2. AERODYNAMIC AND ACOUSTIC EFFECTS OF KEY STRUCTURAL PARAMETERS

This section focuses on the influences of several key structural design parameters on the aerodynamic performance and radiated sound pressure level of the studied multi-blade centrifugal fan combining numerical simulation methods of flow field and far-field radiated noise. The parameter studied includes blade installation angle, number of blades, and the gap between the volute and the blade trailing edge near the volute tongue (volute tongue clearance for short). When one specific parameter is studied, the other two keep unchanged.

Three-dimensional (3D) unsteady-flow numerical simulation of the multi-blade centrifugal fan models is carried out with the computational fluid dynamics software ANSYS CFX. The entire computational domain is divided into two parts: rotating impeller blade domain and stationary volute domain. In consideration of the structural complexity of volute, unstructured mesh cells are constructed by ICEM. Structured mesh is generated for impeller blades. The mesh is refined for blade and volute tongue regions, all blade surfaces, hub wall and volute surface. The total number of the mesh elements is around 7.6×10^6. The fluid region of the impeller blades is set in a rotating reference frame at the rated rotational speed of the multi-blade centrifugal fan, i.e. 600 rpm. The interface between two domains is dealt with sliding mesh model. The inlet is given the ambient total pressure and total temperature, and the outlet is set as static pressure (i.e., back pressure) based on the working condition and system impedance. The scheme of second-order upwind is used for discretization. A steady-flow numerical simulation is computed first to obtain a relatively reasonable flow field. Then this result is used as the initial flow field for further unsteady simulation using the Reynolds averaged Navier-Stokes type k-ε turbulence model with the standard wall function treatment. The residuals of all the parameters fall below 10^{-5}.

Acoustic numerical calculation is conducted with the indirect boundary element method (IBEM) in LMS Virtual.Lab software. With the fluctuating forces on the surfaces of impeller blades obtained from the aforementioned unsteady-flow simulation as input, blades are segmented and each zone is treated as a compact rotating dipole sound source in order to guarantee the accuracy of sound field calculation. The sound field on the surface of a sphere with the spherical radius being 1.414m is analyzed.

2.1 Blade Installation Angle

According to the fan manual, the blade incidence angle of the strong forward-curved centrifugal fan is usually greater than 60° and the exit angle is generally between 150° and 170°. If the incidence angle is too small, the accelerating flow path may be lost and the fan efficiency may decrease. Contrarily, if the incidence angle is too large, the impact loss at the inlet of blades may be too large, and the exit angle is too large, thus the size of the fan is increased under the condition of obtaining equal wind pressure.

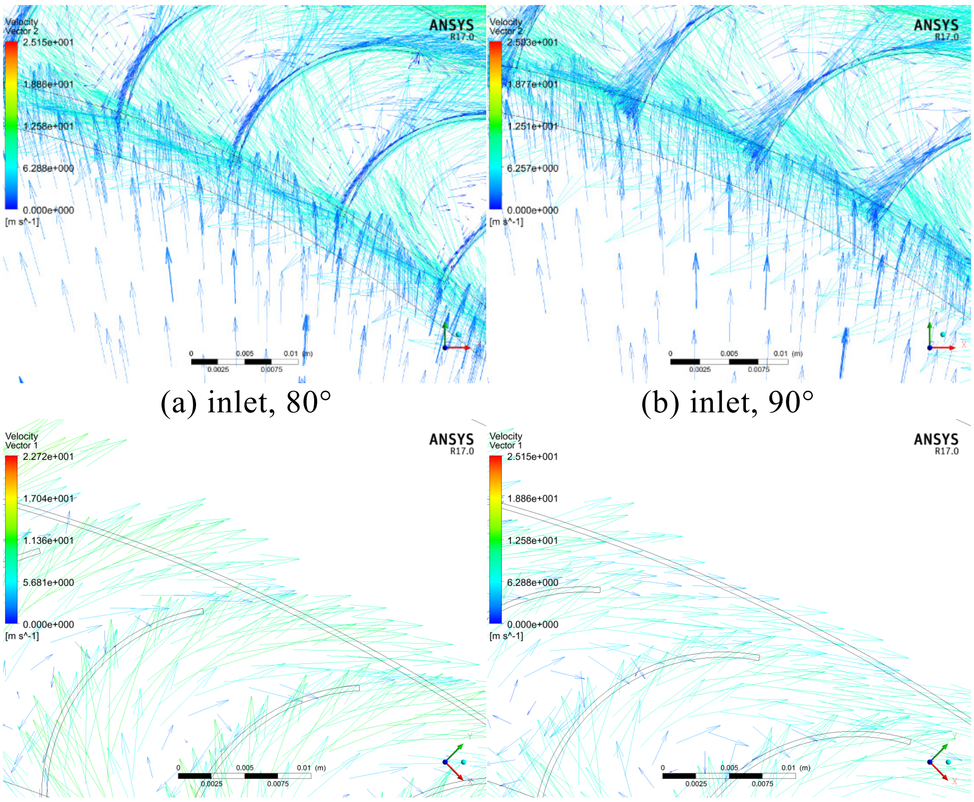

(a) inlet, 80° (b) inlet, 90°

(c) exit, 80° (d) exit, 90°

Figure 1 Comparison of relative velocity vector at the inlet and exit of blades between blade incidence angle being 80° and 90°

Four different blade incidence angles (60°, 70°, 80° and 90°) are explored. In this study, the turning angle (the angular difference between the blade exit angle and the incidence angle) remains unchanged. Thus the exit angle changes with the incidence angle. The flow fields at three typical positions, blade inlet, exit and the flow passage between two adjacent blades, are analyzed. Figure 1 compares the relative velocity vector at the inlet and exit of blades when blade incidence angle equals 80° and 90°.

Ideally, the best condition is the incident angle of the flow equals the geometry incident angle of blades, which means the inlet relative velocity of flow in the rotating reference frame of impeller blades is along the tangent direction of inlet blade profile. Air will flow smoothly into the impeller with the lowest loss. When the inlet flow deviates from the tangent direction of inlet blade profile, an angle of attack will come up. Large attack angle can lead to flow separation and has a bad effect on both aerodynamic and acoustic performance of fans. It can be seen from Fig. 1 that a very large positive angle of attack is formed when the blade incidence angle equals 90°, which causes a large separation vortex in the front part of suction side of blades. When the blade incidence angle is reduced to be 80°, the original positive angle of attack is decreased and the flow separation condition is relieved to some extent.

Figure 2 shows the streamline contours in the flow passage of impeller blades among the four studied blade incidence angles. The airflow velocity distribution along the circumferential direction is very uneven. Separation vortex mainly exists in the regions close to the volute tongue and away from the volute outlet. Secondary vortex phenomenon is more obvious and the airflow is relatively more turbulent in the impeller flow passage with the blade incidence angle being 90°. By contrast, the flow fields of cases of 70° and 80° are organized better.

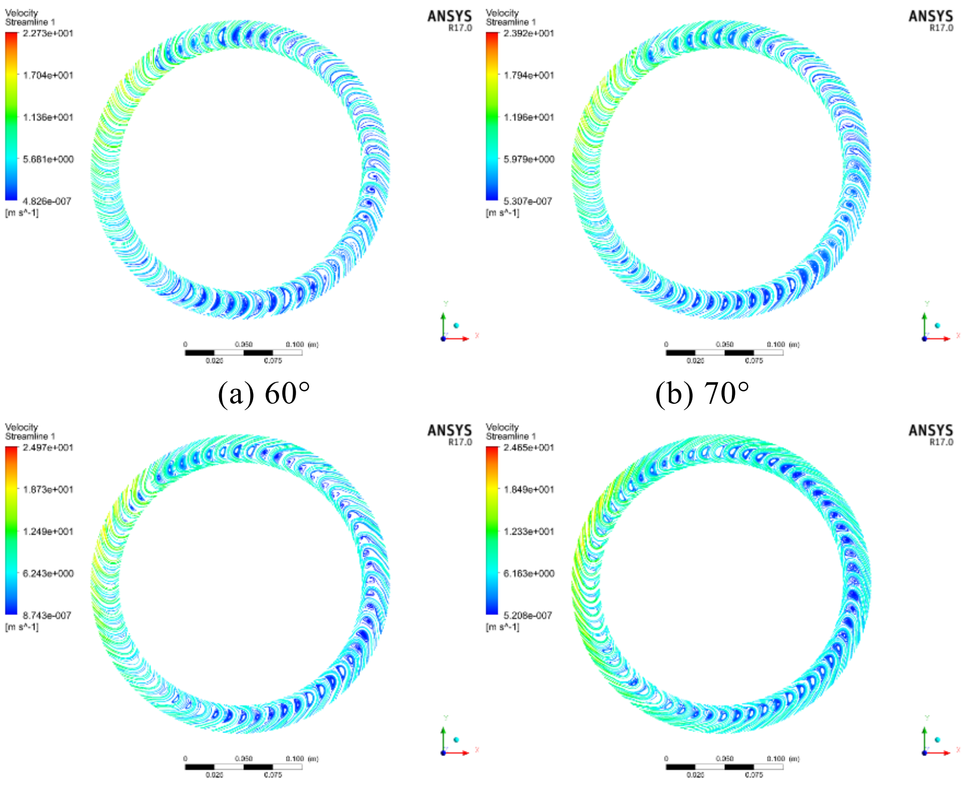

(a) 60° (b) 70°

(c) 80° (d) 90°

Figure 2 Comparison of streamline contours in the flow passage of impeller blades among four different blade incidence angles: (a) 60°, (b) 70°, (c) 80° and (d) 90°. The outlet of volute is located in the left top corner of each figure.

Tables 1 compares air volume flow rate and the maximum value of far-field radiated sound field at the first- and second-order blade passing frequencies (BPFs) among different blade incidence angles. Since the adjustments give rise to little change to the structure of volute and thus the distribution of far-field radiated sound field, it is feasible the highest sound pressure level is selected to compare the acoustic performance. It can be seen that the noise value is the lowest when the blade incidence angle is 70° while the air volume is largest when the blade incidence angle is 80°. This result is consistent with the flow field structure analysis described above.

Table 1 Comparison of air volume and the maximum value of far-field radiated sound field at the 1st and 2nd BPFs among different blade incidence angles

Blade incidence angle (°)	Volume flow rate (m^3/min)	1st BPF (dB)	2nd BPF (dB)
90	17.5	55.2	56.9
80	18.8	59.2	49.5
70	17.8	54.7	49.4
60	17.5	53.9	57.2

2.2 Number of Blade

Similarly, the influence of number of blades on the aerodynamic performance and noise of the centrifugal fan is analyzed. Tables 2 gives the comparison of air volume flow rate and the maximum value of far-field radiated sound field at the first- and second-order BPFs among different blade counts. In the studied range, more blades and higher blade solidity can increase the air volume. However, its influence on tonal noise has no obvious regularity.

Table 2 Comparison of air volume and the maximum value of far-field radiated sound field at the 1st and 2nd BPFs among different number of blades

Number of blades	Volume flow rate (m^3/min)	1st BPF (dB)	2nd BPF (dB)
60	18.8	59.2	56.9
50	18.4	54.7	63
40	17.3	52	49.9

2.3 Volute Tongue Clearance

Tables 3 compares air volume flow rate and the maximum value of far-field radiated sound field at the first- and second-order BPFs among different volute tongue clearances. With the increase of volute tongue clearance, the highest sound pressure levels at the two frequencies are both suppressed (4dB and 4.4dB respectively). In addition, the air volume flow rate is increased by 0.8m^3/min as well.

Table 3 Comparison of air volume and the maximum value of far-field radiated sound field at the 1st and 2nd BPFs among different volute tongue clearances

Tongue clearance (mm)	Volume flow rate (m^3/min)	1st BPF (dB)	2nd BPF (dB)
12.5	16.7	59.2	51.3

18	17.5	55.2	46.9

3. SOUND-ABSORBING VOLUTE DESIGN

3.1 Broadband Sound-Absorbing Structure Design

The sound absorption bandwidth of porous sound-absorbing materials (S.A.M) is usually wide, but its effect on low frequency noise control is very limited. In comparison, the perforated panel absorber can achieve noise control in any frequency band, but the sound absorption bandwidth is narrow. To achieve low-frequency noise control, the thickness of porous sound-absorbing materials needs to be increased, and the depth of the cavity behind the perforated panel needs to increase, which greatly increases the space occupied. In order to achieve both low-frequency and broad-bandwidth noise reduction and reduce the space occupancy, a composite structure is designed by combining the perforated panel absorber and the porous sound-absorbing material based on the analysis of noise spectrum characteristics of the centrifugal fan, illustrated in Fig. 3.

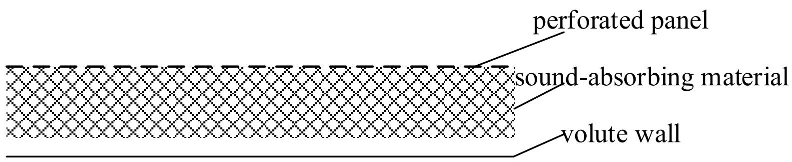

Figure 3 The composite sound absorption structure

The sound absorption coefficient of the perforated panel absorber depends on aperture diameter, perforation ratio, panel thickness and cavity depth. The sound absorption performance of sound-absorbing materials is closely related to its thickness, air flow resistance, porosity, viscous and thermal efficiency characteristic constants. After a systematic study of parametric analysis by restricting the total thickness of 80mm, the optimal parameters are listed in Table 4. The sound absorption performance of the designed composite sound absorption structure is numerically calculated with COMSOL, and its sound absorption coefficient curve is shown in Fig. 4.

Table 4 Structural dimensions and material properties of the composite sound absorption structure

Perforated panel	Aperture diameter	Perforation ratio	Thickness	Cavity depth
	6mm	22%	1mm	30mm
S.A.M	Air flow resistance	Porosity	Viscous/thermal characteristic length	Thickness
	$20000\ \mathrm{Pa\cdot s/m^2}$	89.5%	240/470μm	50mm

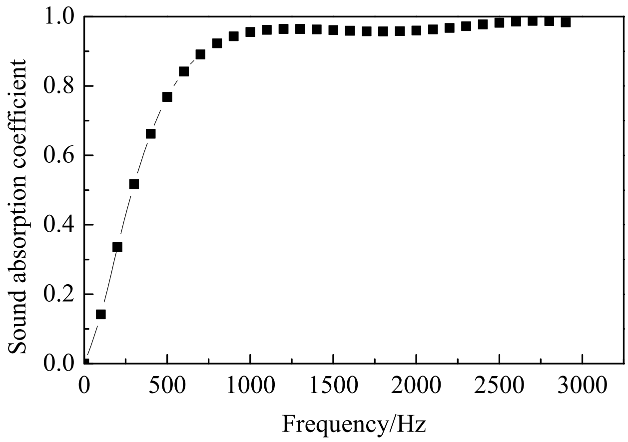

Figure 4 The sound absorption coefficient curve of the composite sound absorption structure

3.2 Effect of Installation Position

Due to the directivity of far-field sound radiation, the adjustment of position where the designed composite sound absorption structure is applied to may have considerable influences on the realistic noise reduction. To validate this, the composite sound absorption structure is installed at three different positions respectively, including all surfaces of volute, only the helical surface of volute and only one lateral side of volute (see Fig. 5). The centrifugal fan model with tongue clearance of 12.5mm, blade incidence angle of 80° and blade count of 60 is selected. The acoustic numerical calculation results of the three cases with LMS Virtual.Lab software are listed in Table 5.

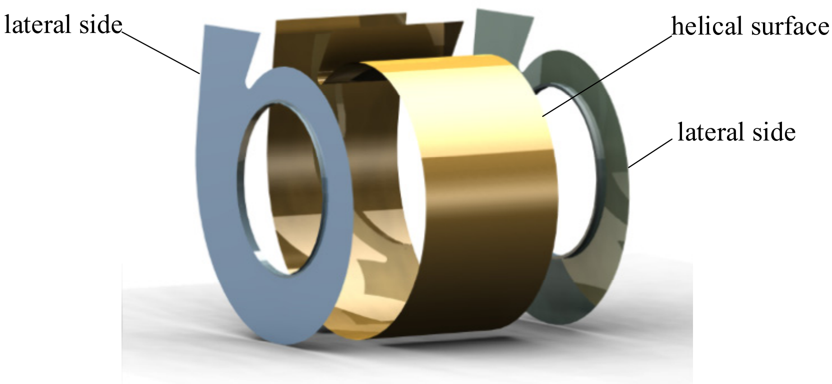

Figure 5 Different installation positions of the composite sound absorption structure

Table 5 Comparison of the maximum value of far-field radiated sound field at the 1st and 2nd BPFs when the designed composite sound absorption structure is applied to different volute surfaces

	1st BPF (dB)	2nd BPF (dB)
All-surface	53.9	44.1
Helical surface	55.5	46.3
One lateral side	56.7	49

The all-surface absorption has the best performance, which is deserved and expected. However, in practical engineering, both noise reduction and the cost need to be taken into consideration, i.e. the benefit-cost ratio. After the designed composite sound absorption structure is applied to the helical surface, the far-field maximum sound pressure level at the first-order BPF is reduced from 59.2dB to 55.5dB, which is 3.7dB lower. For the second-order BPF, this figure is from 49.5dB to 46dB, which is reduced by 3.5dB. This installation position is superior to the lateral side.

3.3 Acoustic Experimental Test

In this section, acoustic experimental test of the multi-blade centrifugal fan after aerodynamic and acoustic improvement is conducted with the global enveloping method. The tested fan is in the center of a sphere with the spherical radius being 1.414m. The selected four monitoring points are uniformly located in the circle formed by intersection of the horizontal plane 1 meter below the center of the sphere with the spherical surface.

For multiple points, the average A-weighted sound pressure level (SPL) in dB(A) is calculated using the formula below:

$$\overline{L}_A = 10\lg\frac{1}{n}\left(10^{0.1L_1} + 10^{0.1L_2} + \cdots + 10^{0.1L_n}\right)$$

where n is the number of monitoring points; L_i is the A-weighted sound pressure level at the ith monitoring point in dB(A).

Noise data at the four monitoring points under different working conditions are measured. The variation of the average A-weighted sound pressure level among the four points with air volume flow rate is plotted in Fig. 6. It can be seen that when the fan flow rate is 15m^3/min, the noise value of the fan is 63.1dB(A), which is 10.9dB(A) lower than the Chinese national standard for range hoods, i.e. below 74 dB(A).

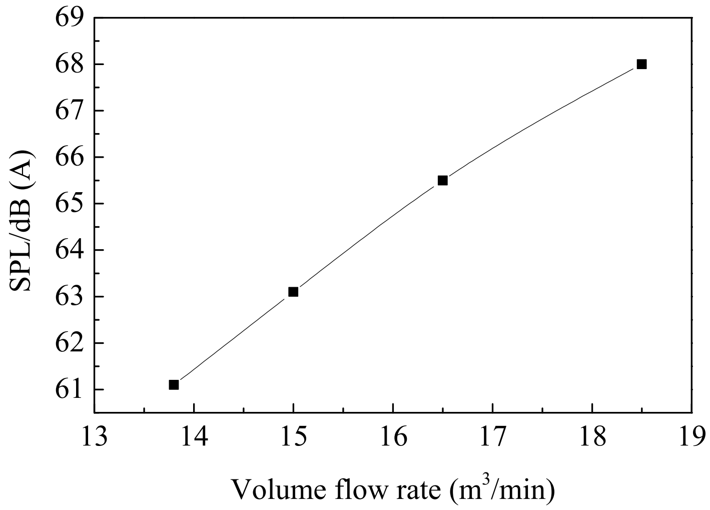

Figure 6 Variation of the average A-weighted sound pressure level among the four points with air volume flow rate

4. CONCLUSIONS

In this paper, the flow field, air flow rate and radiated noise of an existing multi-blade centrifugal fan is optimized through the variation of several key design parameters. The adjustment of blade installation angle, number of blade, impeller blade-tongue gap is beneficial to the improvement of aerodynamic performance and noise control. However, the optimal parameter for aerodynamic performance is not always the optimal one for acoustic performance, and vice versa. A novel composite sound absorption structure is designed and the simulation result shows that it can achieve both outstanding low-frequency and broad-bandwidth noise reduction (above 500Hz) and reduce the space occupancy in the meanwhile. Effect of installation position of the designed composite sound absorption structure in volute wall is explored. In practical engineering, the optimal installation position should be determined base on the directivity of far-field sound radiation and the comprehensive consideration of both benefit of noise reduction and the cost caused.

5. ACKNOWLEDGEMENTS

We acknowledge gratefully Hisense for the support in this research.

6. REFERENCES

1. N. Shimbara, Y. Kodama, H. Hayashi, M. Hatakeyama, "*Characteristics of Fluid Dynamics and Noise of a Multi-Blade Radial Fan (Effects of Inner Diameter and the Number of Blades on the Characteristics of Fluid Dynamics and Noise)*", Transactions of JSME: Part B, 1996, 62(602): 3642-3648.
2. S. Kadota, K. Kawaguchi, M. Suzuki, K. Matsui, K. Kikuyama, "*Experimental Study on Low-Noise Multiblade Fan (1st Report, Visualization of Three-Dimensional Flow between Blades)*", Transactions of the Japan Society of Mechanical Engineers Series B, 1994, 60(570): 452-457.
3. K. Kawaguchi, S. Kadota, M. Suzuki, K. Matsui, K. Kikuyama, "*Experimental Study on Noise Reduction of Multiblade Fan (2nd Report, Relation of Flow between Fan Blades and Pressure Fluctuation)*", Trans. Jpn. Soc. Mech. Eng., Series B, 1994, 60(570): 458-463.
4. K. Morinushi, "*Noise Source of a Multiblade Fan*", Transactions of the Japan Society of Mechanical Engineers, Series B, 1991, 57(543): 3837-3844.
5. S.J. Seo, K.Y. Kim, S.H. Kang, "*Calculations of Three-Dimensional Viscous Flow in a Multiblade Centrifugal Fan by Modelling Blade Forces*", Proceedings of the Institution of Mechanical Engineers, Part A: Journal of Power and Energy, 2003, 217(3): 287-297.
6. S. Velarde-Suárez, R. Ballesteros-Tajadura, J.P. Hurtado-Cruz, C. Santolaria-Morros, "*Experimental Determination of the Tonal Noise Sources in a Centrifugal Fan*", Journal of Sound and Vibration, 2006, 295(3): 781-796.
7. W. Neise, "*Review of Noise Reduction Methods for Centrifugal Fans*", ASME Journal of engineering for Industry, 1982, 104(5): 381-399.
8. S. Velarde-Suárez, R. Ballesteros-Tajadura, C. Santolaria-Morros, B. Pereiras-García, "*Reduction of the Aerodynamic Tonal Noise of a Forward-Curved Centrifugal Fan by Modification of the Volute Tongue Geometry*", Applied Acoustics, 2008, 69(3): 225-232.
9. D. Qi, Y. Mao, X. Liu, M. Yuan, "*Experimental Study on the Noise Reduction of an Industrial Forward-Curved Blades Centrifugal Fan*", Applied Acoustics, 2009, 70(8): 1041-1050.
10. Q. Liu, D. Qi, Y. Mao, "*Numerical Calculation of Centrifugal Fan Noise*", Proceedings of the Institution of Mechanical Engineers, Part C: Journal of Mechanical Engineering Science, 2006, 220(8): 1167-1177.